



Development of an enhanced U-Net model for brain tumor segmentation with optimized architecture

G. Mahesh Kumar^a, Eswaran Parthasarathy^{b,*}

^a Department of Electronics and Communication Engineering, Sumathi Reddy Institute of Technology for Women, Warangal, Telangana 506371, India

^b SRM Institute of Science and Technology, Kattankulathur-603 203, TN, India

ARTICLE INFO

Keywords:

Brain Tumour Segmentation
MRI Image Modality
Enhanced U-Net model
Enhancing Tumour
Whole Tumour
Core Tumour
Adaptive Searched Coyote Optimization Algorithm

ABSTRACT

The paper aims at an enhanced deep learning-based brain tumor segmentation model of MRI images. The input MRI images are pre-processed by the filtering and contrast enhancement techniques, followed by patch extraction. In the pre-processed image, the segmentation of the images is processed by the Enhanced U-Net model; in turn the architecture is optimally tuned by the improved Coyote Optimization Algorithm (COA) called Adaptive Searched Coyote Optimization Algorithm (AS-COA). The hyper-parameters of the U-Net architecture like batch size and the epoch count are optimized by solving the objective function as dice coefficient maximization. The post-processing step includes the morphological closing model for extracting the relevant region of interest with maximum accuracy. The proposed model finally estimates the dice scores for improving whole tumor, tumor and core tumor. Hence, the suggested method's experimental findings demonstrate that it is capable of accurately segmenting brain tumors, as evidenced by comparisons with conventional algorithms.

1. Introduction

The brain represents the major integral parts in central nervous system, which is accountable for the entire human activity. Brain tumors lead to a person's life in jeopardy. The manual work of segmenting the images lead to more time consumption and subjected to many errors [1]. It saves the survival rate of patients by rapid and earlier detection of tumor [2]. Precisely, segmenting the tumors is a significant step with the help of medical images, thereby, it provides the particular region since it exhibits the essential information for analyzing and diagnosing the cancer [3]. For every individual, the shape and appealing nature of brain tumors differ which makes segmentation challenging for radiologists [4]. The brain tumor disorder can cause ailments in a person and death occurs when there are severe conditions [5]. Since the image needs trademark regions, it becomes cumbersome to detect or identify the brain tumor in MRI images [6]. Subsequently, Image segmentation and classification play an essential tool in medical image industry, where the segmentation is performed to extract the affected region and further it is classified into normal and abnormal class pixels [7,8]. Magnetic Resonance Imaging (MRI) becomes an imminent technique used by doctors to assess the existence of malignant and their location. The effectiveness of brain cancer therapy is determined by the skill of the physician. A

brain tumor is characterized by uncontrolled, aberrant cell growth and division, as well as the existence of these immature cell growth [11]. Brain tumors can be classified as either "primary or metastatic tumors". Cells mostly come from brain tissue cells, which are malignant in every other region of the body and proliferate in the brain parts of human. Glioma describes a kind of brain tumor that arises from glial cells [12]. The most deadly and prevalent kind of primary malignant glioma is referred to by this name. The brain tumors having the highest fatality rate and occurrence are gliomas. Patients do not live for more than 14 months following diagnosis, even with therapy. Surgery, chemotherapy, radiation, or a combination of these therapies is now available [13,14].

As it's feasible to generate MRI sequences that provide complementary information, MRI is very beneficial for assessing gliomas in treatment session [15]. For the diagnosis and appraisal of brain tumors, radiologists choose to use MRI. post-contrast T1-weighted (T1ce), T1-weighted, Fluid-Attenuated Inversion Recovery (FLAIR) and T2-weighted are some of the complementary 3D MRI modalities [16 17] that are obtained depending on the degree of repetition and excitation durations. It enables the utilization of these scans in conjunction with the additional information they provide to detect various tumor sub-regions [18]. Manually defining brain tumor sub-regions from MRI

* Corresponding author.

E-mail addresses: mahival2002@gmail.com (G. Mahesh Kumar), eswaranp@srmist.edu.in (E. Parthasarathy).

<https://doi.org/10.1016/j.bspc.2022.104427>

Received 28 July 2022; Received in revised form 11 November 2022; Accepted 20 November 2022

Available online 2 December 2022

1746-8094/© 2022 Elsevier Ltd. All rights reserved.

data describes a subjective procedure that takes time and is liable to error. On the medical side, radiologists may encounter the issue of determining the nuclei of brain cells from the substance of an MRI image [19]. Currently, owing to the shape and position of tumors in the brain while employing multi-modality images, segmenting brain tumors from MRI images can be a tough task. As a result, image segmentation may be the most difficult aspect of tumor identification in the case of a brain MRI image. However, tumor segmentation, as well as separation, are critical for accurate diagnosis and identification of brain tumors [20]. The right segmentation procedure can provide qualitative and quantitative data on a benign tumor or a malignant tumor, which can be used to determine what the best therapies are for the patient and to help the doctor who serves the patient develop a better strategy. When image analysis is simple to grasp and segment, efficient tumor identification may be achieved. As a result of the difficult tumor segmentation stage in MRI images, several algorithms and approaches for manual, semi-automatic, and fully automated tumor segmentation have been developed.

As a result, automated glioma segmentation from multimodal MRI scans can help clinicians quicken surgical planning and diagnosis as well as offer an appropriate, repeatable option for future tumor study and monitoring [21]. Feature engineering is used in traditional techniques of automated brain tumor segmentation, which entails extracting hand-made features from input images and then training a classifier [22]. By autonomously establishing a hierarchy of feature representations, unsupervised learning algorithms circumvent the difficulty of developing and selecting features, with deep learning methods excelling at the task. Convolutional Neural Networks (CNNs) [23] are deployed for obtaining brain tumor images because they automatically train the most valuable and significant information. Owing to the variety concerning form, tumour size, and presence of gliomas, an also unclear and fuzzy peripheral that exists among brain and cancer tissue [24–25], effective tumor segmentation continues a difficulty. The MRI data's intensity fluctuation just adds to the challenge. As a result, it may still be improved, permitting more research into better segmentation approaches and accuracy.

In 2019, Pereira et al. [1] have created a CNN-based automated segmentation approach that explored tiny 3×3 kernels. The usage of tiny kernels has permitted for the creation of a more complex architecture, as well as a reduction in over fitting due to the reduced amount of weights present in the network. The utilization of intensity normalization as a pre-processing phase, which previously not popular in CNN-oriented segmentation algorithms, has proven to be particularly successful for brain tumour segmentation in MRI images when combined with data augmentation. The generated model was verified in the "Brain Tumor Segmentation Challenge 2013 database (BRATS 2013)", achieving first place in the Dice Similarity Coefficient measure for the Challenge data set for the whole, core, and enhanced regions. In addition, the online evaluation platform has given it the global first place.

In 2020, Deng et al. [2] have proposed an approach in which a framework was created to identify and order tumour types. Several experts have been studied and a method presented in this domain over a period of years. Heterogeneous CNNs (HCNN) and Conditional Random Fields (CRF) were used to construct a brain tumour segmentation solution on the basis of efficient, deep learning approaches deployed in a unified system to accomplish the spatial accuracy and appearance objectives. The deep-learning method's 2D image patching and image slicing were produced during these phases. The steps in the suggested technique were as below: 1) image patches were used to train HCNN; 2) image slices having constant variables of HCNN were used to train CRF with CRF-Recurrent Regression based NN (RRNN); and 3) image slices having CRF-RRNN and HCNN were used to train CRF having CRF-RRNN. Generally, three segmentation methods were trained by coronary, axial, and sagittal imaging slices and patches, then merged into brain tumour segments with the help of a voting fusion approach and tested on the Internet of Medical Things (IoMT) Platform. The experimental findings

showed that the suggested method was capable of building a T1c, Flair, and T2 segmenting method and getting satisfactory outcomes with Flair, T1c, T1, and T2 scans.

In 2020, Ali et al. [3] have combined two segmentation networks, a U-Net and a 3D CNN, in a major but simple combinative method that has led to improved and more appropriate predictions. Both methods were trained individually on the BraTS-19 challenge dataset and assessed to produce segmentation maps that varied significantly with respect to segmented tumour sub-regions and were ensemble in different ways to arrive at the final prediction. On the validation group, the proposed ensemble received high dice scores, outperforming conventional designs.

In 2019, Razzak et al. [4] have built a new model two-pathway-group CNN architecture for brain tumour segmentation, that leveraged both local as well as global environmental data at the same time. To prevent over fitting parameter sharing and instabilities, this approach imposed equivariance in the two-pathway CNN model. Moreover, the suggested model incorporated a cascade architecture into a two-pathway-group CNN, with the output of a fundamental CNN being considered as an extra source and combined at the final layer. The model was validated using the "BRATS2013 and BRATS2015 data sets", and it was discovered that integrating a group CNN into a two route architecture enhanced overall performance over the conventional methods while keeping computational complexity low.

In 2019, Thillaikkarasi and Saravanan et al. [5] have combined M-SVM with a revolutionary deep learning technique to automatically and accurately segregate the tumour. There were multiple processes, including "preprocessing, feature extraction, image classification, and brain tumour segmentation". The tumour form location, shape, and surface characteristics in the brain were used to smooth and improve the MRI image using the "Laplacian of Gaussian filtering method (LoG) with Contrast Limited Adaptive Histogram Equalization (CLAHE)", and features were recovered from it. As a result, M-SVM was used to classify the images based on the characteristics that were chosen. The tumour was segmented from an MRI image using a kernel-oriented CNN approach. In comparison to traditional algorithms, experimental findings of the suggested method showed that it properly segmented brain tumours with an accuracy of about 84 percent.

In 2021, Pitchai et al. [6] have used a mix of Fuzzy K-means and Artificial Neural Networks method for segmenting the tumour location. "(1) Noise evacuation (2) Attribute extraction and selection (3) Classification and (4) Segmentation" were the four processes. The obtained image was first denoised with a Wiener filter, and then the important GLCM properties were extracted from the images. The aberrant images were then classified from the normal ones using Deep Learning-oriented classification. Next, it was subjected to the Fuzzy K-Means method, which allowed the tumour region to be segmented individually. When contrasted to the K-Nearest Neighbor strategy, the overall accuracy of the suggested strategy has enhanced by 8 %.

In 2021, Ramya et al. [7] have created an image segmentation ensemble approach to segment the tumour area of a brain MRI image. The images were pre-processed using the Laplacian cellular automata filtering technique, and then segmented using an ensemble of distinct clustering techniques, including "K-means, fuzzy based clustering, Self-Organization Map (SOM), and an ensemble of Gaussian mixture model, K-means, and SOM", with the outcomes compared. Through the deep super learning approach, this ensemble cluster label was regarded the segmentation outcome and has categorized the anomalies. The experimental findings and comparison charts have determined the suggested method's performance rate in comparison to remaining approaches.

In 2021, Jiang et al. [8] have addressed DDU-net that was a novel dual-stream decoding CNN architecture paired with U-net for automated brain tumour segmentation on MR images. To improve the performance of brain tumour segmentation, two edge-oriented optimization algorithms were applied. To commence, a new branch was created to handle edge stream data. In this case, high-level edge characteristics were

lowered in channel size and residually merged into the ordinary semantic stream. Secondly, by compensating pixels in which the forecasted segmentation masks and labels did not match when surrounding the edge, a regularization loss function was employed to induce the forecasted segmentation mask to coincide with ground truth across the edge. A unique edge extraction technique was used in training to provide higher-quality edge labeling. Furthermore, in the back propagation, a “self-adaptive balancing class weight coefficient” was introduced to solve the major class imbalance conflict. Experiments have demonstrated that this resulted in a highly effective design that could generate more accurate predictions near the tumor’s edge.

The robustness and accuracy of brain tumor segmentation has many challenging tasks, and so, it is considered to be crucial for diagnosing and treatment outcome evaluation. Therefore, deep learning approach are taken for automatically extracting the features in the recent development model of tumour segmentation that is illustrated in Table 1. CNN [1] is simple for training and also ensures less probability of undergoing overfitting problems. Yet, it requires more sample images for training the network. HCNN and CRF-RRNN [2] provide high robustness on segmentation in terms of the training images and its patch size. However, it is slow and complexity occurs while training the data. U-Net and CNN [3] increases the segmentation accuracy of enhancing tumor class by replacing the region with a set threshold for necrosis. But, it has been verified only on the “official validation set of challenge” but not considered the separate clinical MRI data. 2PG-CNN [4] ensures less computational complexity and also minimizes the instability and overfitting problems. On the other hand, the training process gets affected and results in unbalancing in them due to overwhelming healthy patch count. CNN with M-SVM [5] provides high accuracy with low time complexity and error rate for segmenting and classifying the brain tumor. At the same time, It does not perform better when processing large datasets and causes overlapping problems. ANN and CSOA [6] achieve improved segmentation results with high accuracy along with increased SSIM value. However, this model lacks the detection of other types of diseases through segmentation and classification. DSL [7] identifies the abnormality class accurately, which is observed through the analysis of the feature vector of the segmented tumor. DDU-net [8] overcomes the serious class imbalance problem that is caused due to the back propagation of edge extraction. But, it is highly concentrated only on the edge features and does not focus on other features for segmentation. Therefore, a novel brain tumor segmentation developed by deep learning technique is necessary to solve the conventional problems of segmentation.

This paper’s contributions are to.

- Enhance a deep learning-aided brain tumour segmentation model for MRI images by gathering the images from publically available sources.
- Segment the images for three tumour regions like “whole tumour, enhancing tumour and core tumour” by the Enhanced U-Net model, where the parameters such as epoch count and batch size are optimized with the consideration of dice coefficient maximization.
- Propose an optimized algorithm called AS-COA for improving the segmentation phase of the suggested brain tumour segmentation model and compare it with distinct heuristic-based and existing segmentation-based algorithm’s to describe the model’s superiority.

The paper organization is as follows. Section I explores the fundamentals of brain tumour segmentation model. The survey works are given in Section II. Section III gives the enhanced DL-based brain tumour segmentation. The optimizing U-Net architecture using AS-COA is explained in Section IV. Section V defines the developing novel brain tumour segmentation using the optimized architecture of U-Net. Section VI contains experimental results and its discussions. The research paper is enclosed in Section VII.

2. Enhanced deep learning-based brain tumor segmentation

2.1. Proposed architecture

MRI is a commonly used medical tool for detecting cancers and diagnosing different tissue abnormalities. Assessing tumour development, treatment process, treating the patients by radiation therapy, computer-aided surgery and building tumour developments are all reasons for segmenting brain tumours. As a consequence, computer-aided diagnostic systems are useful in medical treatments since they reduce doctors’ effort while also providing reliable findings. Owing to their considerable variation in form, position, and appearance, they might be challenging to identify and define using traditional manual segmentation. Furthermore, manual annotation of tumour tissue segmentation requires constant supervision from a human specialist, which requires more time and tiresome. Automatic segmentation, as well as survival rate forecasting methods, will aid in more appropriate and timely treatment and diagnosis. Nowadays, deep learning has conquered the majority of the tasks in medical image analysis, such as segmentation and tracking. It has been used in several types of research for brain tumour segmentation as well as survival prediction. The survival days for every patient are shown in the computed majority of cases by retrieving shape as well as geometrical features, combining them with informative features of clinical information, and training to validate the performance by distinct regression approaches such as “Support Vector Machine (SVM), Artificial Neural Network (ANN), Random Forest, XGBoost”, and others. Data augmentation and improvement of patch extraction techniques and network hyper-parameters are frequently used to improve segmentation performance. In practice, though, achieving a single “optimal” model is extremely difficult, any model might suffer from random mistakes. An ensemble of several methods, identical to standard machine learning tasks, may normally enhance segmentation accuracy since separate concepts may make various mistakes, and the ultimate count of errors can be decreased by majority voting or averaging. The very varied look and form of brain tumours, involving sub-regions, make segmentation difficult, which can be exacerbated by imaging errors like motion and/or field inhomogeneity. The architectural representation of the suggested brain tumour segmentation model is shown in Fig. 1.

The proposed brain tumour segmentation model covers mainly-four phases are, “data collection, pre-processing, segmentation, and post-processing”. Initially, the MRI images are downloaded from the standard benchmark sources. These images are given to the pre-processing step that is undergone via filtering, patch extraction and contrast enhancement techniques.

Next, the pre-processed images are subjected to the segmentation process, which is done with the help of U-Net. Here, the batch size, as well as the number of epochs, is of U-Net are optimized by AS-COA with the consideration of dice coefficient maximization thus called as enhanced U-Net. Here, the segmentation is done for three regions such as whole tumour, enhancing tumour and core tumour. Further, the post-processing of each segmented region is done by morphological closing. The segmentation maps from these three regions after post-processing is combined to return a final segmented output for the type of tumour tissue. This, in turn finally estimates the dice scores relied on whole tumour, enhancing tumour, and core tumour.

2.2. Description of datasets

The dataset used for the enhanced brain tumour segmentation model is the “Brain-Tumor_Segmentation_BraTS_2019” dataset [35]. The entire imaging datasets were segmented in a manual format and rated with a range from first to fourth by annotation technique, in which its annotations were revised and validated by best neuroradiologists. The gadolinium enhancing tumour, the “peritumoral edema, and the necrotic and non-enhancing tumour core” are included in the

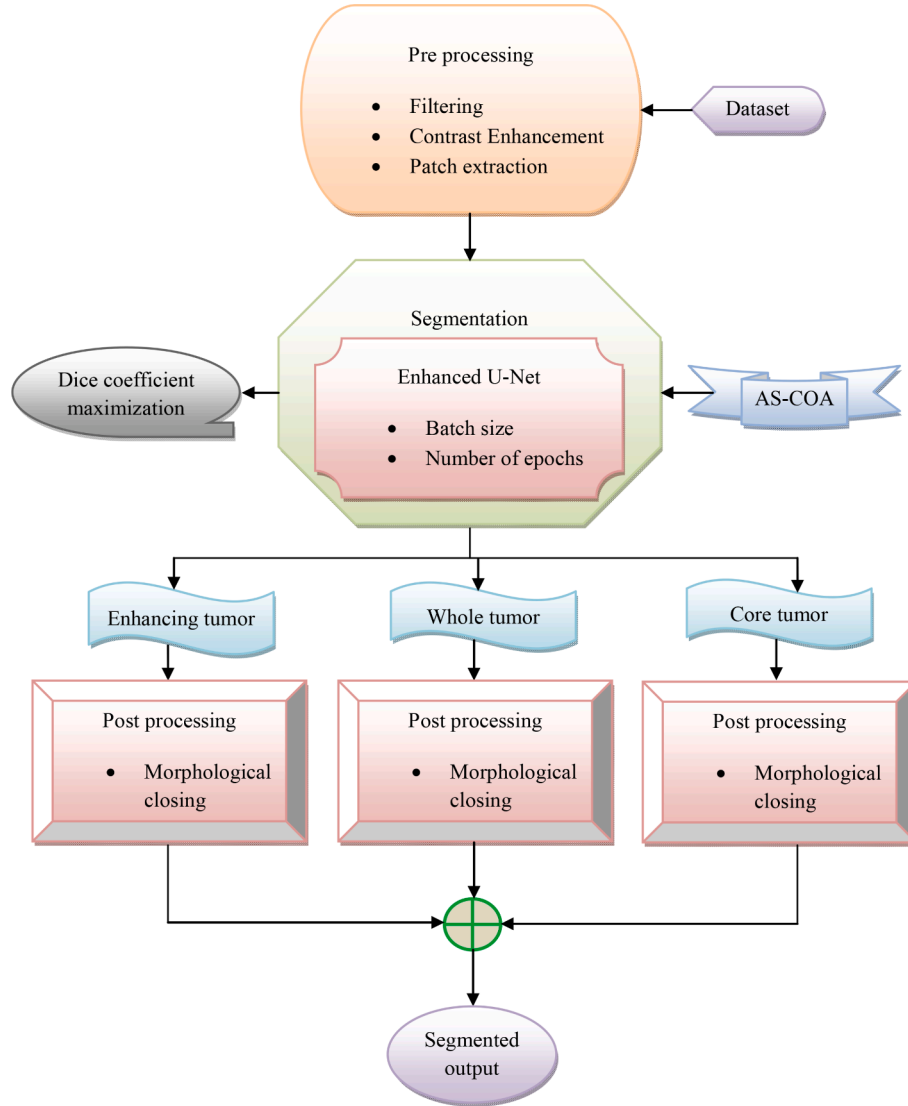


Fig. 1. The architecture of the proposed brain tumor segmentation model.

annotations. The different organization dataset obtained from 19 distinct contributors is composed of multimodal MRI scans of every patient such as, “T1, T1 contrast-enhanced (T1 ce), T2-weighted (T2), and Fluid Attenuated Inversion Recovery (FLAIR)” from where the segmentation of tumoral subregions occurs. Once the pre-processing is done, the image is disseminated, which includes “co-registration to the same anatomical template, interpolation to the same resolution, and skull-stripping”. Some of the sample images from the considered dataset are shown in Fig. 2.

2.3. Pre-processing of input MRI images

To eliminate undesired artifacts and convert the data into a standard format, functional fMRI data must be pre-processed. It is accomplished by resizing and orienting the images, and colour adjustments, with respect to other characteristics. The transformation is mostly done in the pre-processing phase for avoiding the complexity that occurs mostly in the further steps. Here, the pre-processing is done by filtering, contrast enhancement, and patch extraction techniques. The dataset is specified as L_s^{in} , where $s = 1, 2, \dots, S$, in which S signifies the entire images of dataset.

Filtering: Median filter is used here to preserve the sharp edges. A nonlinear filtering strategy for decreasing noise in input images is

described by the median filtering approach [27]. Assume that the input vector is L_s^{in} and the median filter output is L_s^{med} , with length lv and sample count $asnv$. When it is shown to be odd lv , Eq. (1) [27] determines the median filter.

$$L_s^{\text{med}}(nv) = \text{median}\{L_s^{\text{in}}(nv - kv : nv + kv), \quad kv = (lv - 1)/2\} \quad (1)$$

The contrast enhancement is used to further improve the image quality after the final median filtered image is obtained which is represented as L_s^{med} .

Contrast Enhancement: Contrast enhancement [28] is a frequently used technique in image processing to increase the dynamic range. The common histogram variation approach is used to provide a wide dynamic range. Fixed histogram techniques offer two different benefits: they level the histogram and increase the dynamic range. Grey levels falls in the range of $[0, LU - 1]$ are examined in a digital image. Eq. (2) [28] shows the “Probability Distribution Function (PDF)”.

$$PU(ru_{ku}) = \frac{nu_{ku}}{NU} \quad ku = 0, \dots, LU - 1 \quad (2)$$

In the Eq. (2), the pixel count is supplied as nu_{ku} and the grey level is defined by ru_{ku} . Eq. (3) [28] is used to compute the “Cumulative Distribution Function (CDF)”.

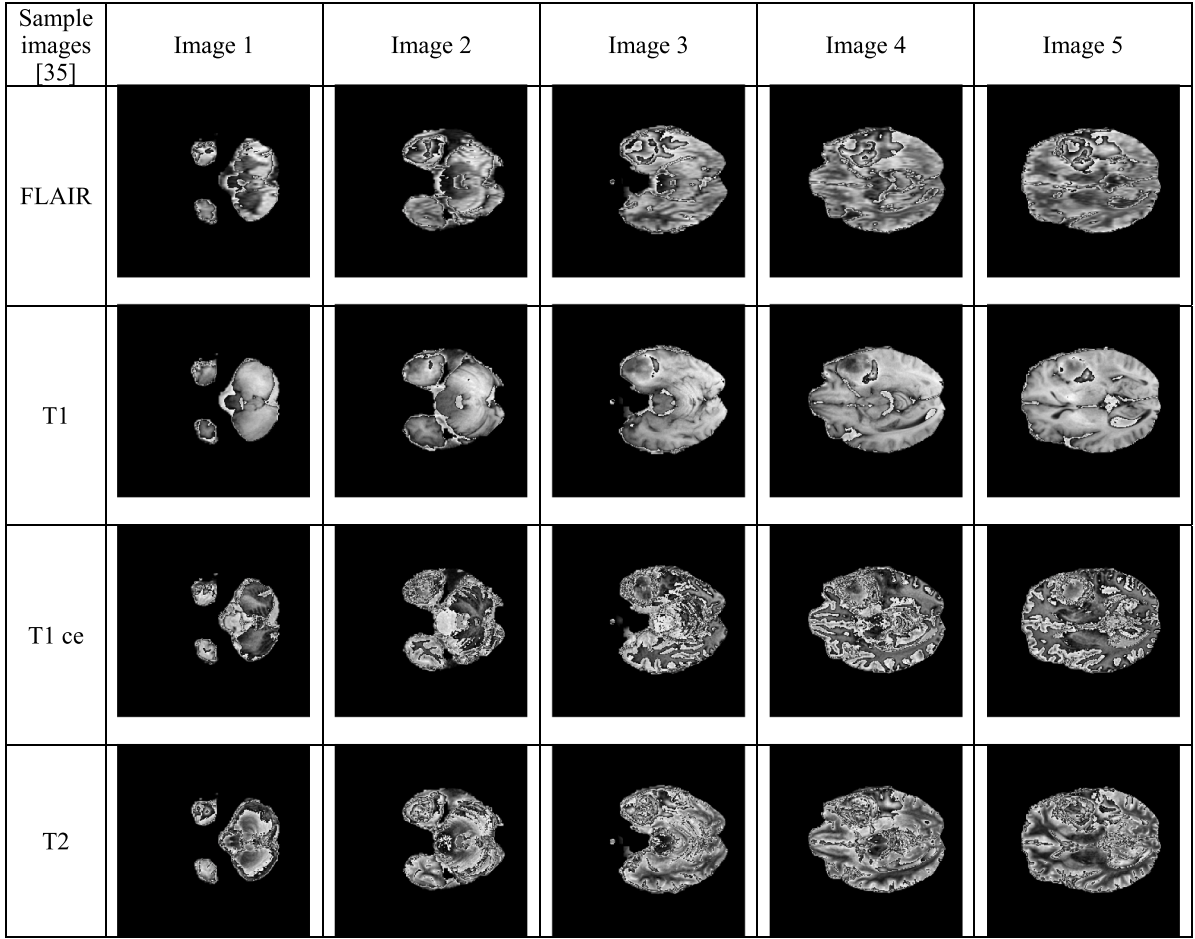


Fig. 2. Sample images in the dataset for the suggested brain tumour segmentation model.

$$CU(ru_{ku}) = \sum_{iu=0}^{iu=ku} PU(ru_{iu}) \quad (3)$$

$$ku = 0, \dots, LU - 1, \quad 0 \leq CU(ru_{ku}) \leq 1$$

The grey level in this equation SU_{ku} differs from the grey level ru_{ku} in Eq. (4) [28].

$$SU_{ku} = (LU - 1) \times CU(ru_{ku}) \quad (4)$$

Eq. (5) [28] closely resembles the grey level fluctuations SU_{ku} in the standard histogram equalisation technique.

$$\Delta SU_{ku} = (LU - 1) \times PU(ru_{ku}) \quad (5)$$

As a result, L_s^{con} is a contrast-enhanced image.

Patch extraction: In the patch extraction technique, the subtraction takes place with the aid of every pixel's value and patch's mean. Here, patches are arranged by its computed energy level, in which higher level

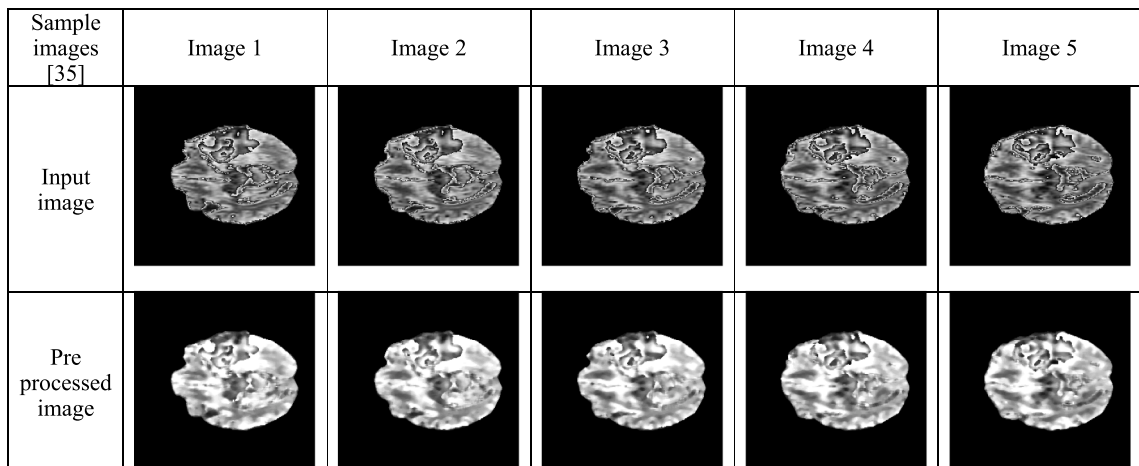


Fig. 3. Sample pre-processed images for the suggested brain tumour segmentation model.

of energy is fixed via thresholding. Columns are created by reshaping patches. Here, the final pre-processed image is shown by L_s^{pre} and it is given to the segmentation step for further processing. Sample of pre-processed images for the suggested brain tumour segmentation model is shown in Fig. 3.

3. Optimizing U-net architecture using an improved coyote optimization algorithm

3.1. Conventional COA

The COA [26], a novel *meta*-heuristic method, has been devised. The method is dependent on the distribution of experience and the coyote's contextual adaption behavior. COA has devised a unique technique to strike a balance between exploitation and exploration. As there are many possible solutions, the process starts with a Q_s population census and an Q_f estimate of coyotes. The COA uses a cost function to describe coyote social behavior. In this sense, the social features of a coyote are as follows [26]:

$$SE_f^{s,w} = a = [a_1, a_2, \dots, a_G] \quad (6)$$

Here, f means the number, s displays the group, and w specifies the simulation duration for the model parameters. Originally, a large number of arbitrary coyotes were formed as solution candidates in the search space. This process design may be seen in the equation as follows [26].

$$SE_{f,m}^{s,w} = LB_m + \eta \times (UT_m - LT_m) \quad (7)$$

In the previous equation, $\eta \in [0, 1]$ denotes a random value, whereas LT_m and UT_m denote the bottom and upper ranges of the m^{th} factor in search space, respectively. Following are the cost functions [26] for each coyote.

$$FV_f^{s,w} = h(SE_{f,m}^{s,w}) \quad (8)$$

The groups are shuffled at random by the algorithm. Furthermore, the applicants' positions alter as they move from one group to the next. The procedure of departing is summarised in the below equation [26], which is predicated on the probability formulation.

$$S_o = 0.05 \times Q_f^2 \quad (9)$$

The alpha coyote, which is determined using Eq. (10) [26], describes the best solution for every iteration.

$$\alpha^{s,w} = se_f^{s,w} \text{ for } \min FV_f^{s,w} \quad (10)$$

Eq. (11) [26] depicts the coyote's common characteristics in terms of cultural tendency.

$$cn_m^{s,w} = \begin{cases} U_{\frac{Q_f+1}{2}-m}^{s,w} & Q_f \text{ is odd number} \\ \frac{1}{2} \left(U_{\frac{Q_f}{2}-m}^{s,w} + U_{\frac{Q_f+1}{2}-m}^{s,w} \right) & O.W. \end{cases} \quad (11)$$

The coyotes' social status is examined by rating the group count s at timestamp w is supplied by $U^{s,w}$ in the case of a variable m . The COA examines the life style behaviour of the coyote, which is impacted by both environmental conditions and parental coyote features. The life cycle is depicted in Eq. (12) [26].

$$Bg_m^{s,w} = \begin{cases} se_{u1,m}^{s,w}, & u_m < qu_v \text{ or } m = m_1 \\ se_{u2,m}^{s,w}, & u_l \geq qu_v + qu_d \text{ or } m = m_2 \\ \sigma_n, & O.W. \end{cases} \quad (12)$$

The term $u_m \in [0, 1]$, a random value is denoted by u_2 and s indicates a

random coyote in the group, σ_m indicates a random value inside the design variable limit m_1 , m_2 refers the variables arbitrarily, qu_d and qu_v depicts the cultural variety of the coyote. Eqns. (13) [26] and (14) [26] illustrate the mathematical formulations for qu_d and qu_v .

$$qu_v = \frac{1}{g} \quad (13)$$

$$qu_d = \frac{1}{2}(1 - qu_v) \quad (14)$$

Here, g defines the dimension of variables in the given equations. The two elements reflect the cultural shift within the groups δ_1 and δ_2 are defined by Eq. (15) and Eq. (16) [26].

$$\delta_1 = \alpha^{s,w} - se_{du1}^{s,w} \quad (15)$$

$$\delta_2 = cn^{s,w} - se_{du2}^{s,w} \quad (16)$$

Here, δ_1 illustrates the cultural differences among the chosen coyote $du1$ and its leader is represented by the word "alpha", as well as δ_2 gives the cultural contrasts between the moving group culture and the picked coyote $du1$. Eq. (17) [26] has been used to adjust social features throughout the leader and group influence.

$$qse_f^{s,w} = se_f^{s,w} + u_1 \times \delta_1 + u_2 \times \delta_2 \quad (17)$$

In the above equation, the two arbitrary values as u_1 and u_2 lies in the range of $[0, 1]$. Eq. (18) [26] and (19) [26] are used to determine the new cost after analyzing the updating equations.

$$qFV_f^{s,w} = h(qse_f^{s,w}) \quad (18)$$

$$se_f^{s,w+1} = \begin{cases} qse_f^{s,w}, & qFV_f^{s,w} < FV_f^{s,w} \\ se_f^{s,w}, & O.W. \end{cases} \quad (19)$$

The capacity to escape from the local ideal position is a key feature of these approaches.

3.2. Proposed AS-COA

The proposed AS-COA is developed for enhancing the segmentation phase of the developed brain tumour segmentation model through the optimization of the parameters of U-Net such as number of epochs and its batch size is taken into the consideration of dice coefficient maximization. The traditional COA provides several key points, entails with improved exploration and exploitation, enhanced searching capabilities, and so on. It does, however, avoid drawbacks such as early convergence owing to population selection in a random manner, long-term of running time, etc. To get over these limitations, the random numbers are revised using a superior concept known as AS-COA. This AS-COA has several advantages, including avoiding early convergence and saving time.

In the conventional COA, the variables like u_1 and u_2 lies in the range of $[0, 1]$. On the contrary of introduced AS-COA, the defined random numbers are computed based on adaptive search as in Eq. (20).

$$u_1, u_2 = \frac{j+1}{Npop} \quad (20)$$

Here, the term j represents the index and the population size is given by $Npop$ respectively. Further, in the traditional COA, the cultural tendency is computed by the median of the coyote position. But, in the proposed AS-COA, the cultural tendency is calculated by the mean of the coyote position as in Eq. (21).

$$cn_m^{s,w} = \text{mean}(se_f^{s,w}) \quad (21)$$

The pseudo-code of the introduced AS-COA is in Algorithm 1, and its flowchart is in Fig. 4.

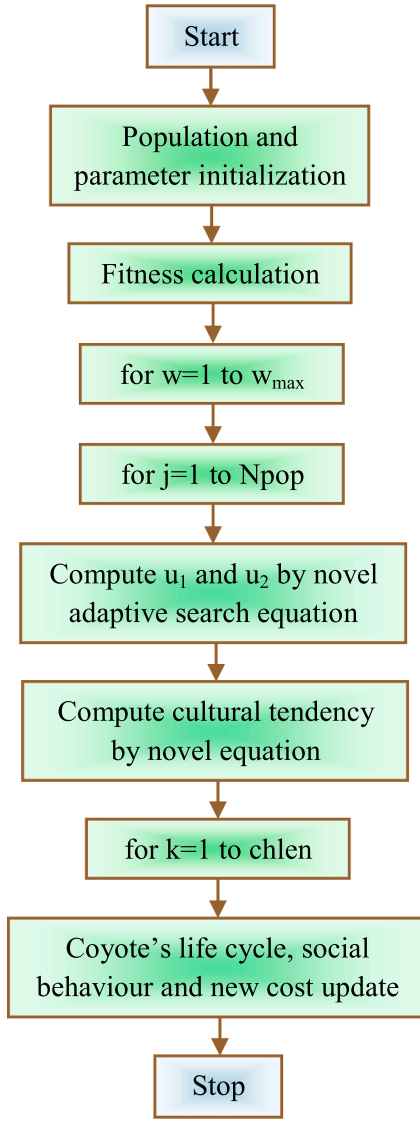


Fig. 4. Proposed AS-COA process flow.

Algorithm 1: Proposed AS-COA

```

Begin
Set the population and its parameter
Determine the fitness value
For w = 1 to w_max
  For j = 1 to Npop(population size)
    Compute  $u_1$  and  $u_2$  by novel adaptive search equation as in Eq. (20)
    Compute cultural tendency in Eq. (21)
    For k = 1 to chlen(chromosome length)
      Coyote's life cycle update through Eq. (12)
       $\delta_1$  and  $\delta_2$  update through Eq. (15) and Eq. (16)
      Coyote's social behaviour update through Eq. (17)
      Coyote's new cost update through Eq. (19)
    End
  End
End
End
Stop
  
```

4. Developing novel brain tumor segmentation using the optimized architecture of U-Net**4.1. U-net model**

The proposed brain tumor segmentation and classification model uses U-Net-oriented segmentation to segment the pre-processed images. U-Net segmentation describes a supervised approach that accurately extracts the provided area using a training program and a mask obtained manually. The AS-COA is recommended for fine-tuning the number of epochs and batch sizes. The U-Net design [29] is built of two paths: one that expands and the other that contracts. The contracting route is used to process the convolutional network. The “cropped feature map and the two 3×3 convolutions” make up the structure. Cropping is required since lack of boundary pixels in every convolution process. Every “64-component feature vector in the final layer” translates the 1×1 convolution to the desired class count.

A stochastic gradient descent approach is used to train the network by the input images and segmentation. “At the pixel location $xx \in \Omega$ having $\Omega \subset \mathbb{Z}^2$, the activation function in the feature channel kx ” is defined by $ax_{kx}(xx)$ and the soft-max is offered as $px_{kx}(xx) = \exp(ax_{kx}(xx)) / (\sum_{kx'=1}^{KX} \exp(ax_{kx'}(xx)))$. The class count is marked as KX and the anticipated maximum function is denoted as $px_{kx}(xx)$ and $px_{kx}(xx) \approx 1$ for kx that includes the maximum activation $ax_{kx}(xx)$ and $px_{kx}(xx) \approx 0$ for the remainder kx . Each deviation point $px_{kx}(xx)$ from 1 is dealt with by the cross functions, as illustrated in Eq. (22).

$$EX = \sum_{xx \in \Omega} wx(xx) \log(px_{kx}(xx)) \quad (22)$$

The real pixel labels are defined as $lx : \Omega \rightarrow \{1, \dots, KX\}$, while a weight map is added with few pixels that provides the substantial information in the training phase, which is signified by $wx : \Omega \rightarrow \mathbb{R}$. “Each ground-truth segmentation’s weight map is pre-computed to compensate for the unique pixel frequency of a certain class in the training group, and to push the network to investigate the small separation, “boundaries that are suggested inside the contacting cells”. Morphological techniques are deployed to determine the separation boundary. Using Eq. (23), the weight map is computed.

$$wx(xx) = wx_{cx}(xx) + wx_0 \cdot \exp\left(-\frac{(dx_1(xx) + dx_2(xx))^2}{2\sigma^2}\right) \quad (23)$$

The “distance to the border of the second closest cell” here is $dx_2 : \Omega \rightarrow \mathbb{R}$, the “distance to the border of the first closest cell” is $dx_1 : \Omega \rightarrow \mathbb{R}$, and the weight map for managing the class frequencies is $swx_{cx} : \Omega \rightarrow \mathbb{R}$. The initial weights are calculated using a “Gaussian distribution with a standard deviation” of $\sqrt{2/NX}$, wherein NX is the input node count belongs to single neuron. Here, the segmentation is done for three regions such as enhancing tumour, whole tumour, and core tumour, and they are represented by L_s^{enh} , L_s^{who} , and L_s^{cor} respectively.

4.2. Enhanced U-Net-based segmentation

Using the parameter optimization of U-Net by the suggested AS-COA, the enhanced U-Net-aided brain tumor segmentation is employed for segmenting the brain tumor images. According to the AS-COA method, an objective model based on dice coefficient maximization should be used. Since this U-Net performs image segmentation, the dice coefficient is an important parameter in the objective model.

The U-Net provides several benefits, involving the capability to employ the context information of local and global at the same time, as well as functions that need minimum training data. Nevertheless, it is limited by the fact that it drops off in the mid process of more advanced approaches, and so on. Consequently, the AS-COA optimizes “batch size and epoch count” to mitigate the drawbacks. This enhanced U-Net offers several

benefits, involving the capacity to accept images of varied sizes and excellent efficiency. As a result, the main objective of U-Net-based brain tumor segmentation is provided in Eq. (24). The bounding limit for batch size is 1000 to 5000, while the bounding limit for epoch count is 1 to 5.

$$Of = \underset{\{BS_{U-Net}, EC_{U-Net}\}}{\operatorname{argmin}} \left\{ \frac{1}{Dice} \right\} \quad (24)$$

Here, the fitness function for the segmentation is shown by Of , the batch size is shown by BS_{U-Net} , epoch count is shown by EC_{U-Net} and the dice coefficient is shown by $Dice$ respectively. Dice coefficient is defined as, “measuring the overlap between the manual and the automatic segmentation” as in Eq. (25).

$$Dice = \frac{2T^p}{F^p + 2T^p + F^N} \quad (25)$$

In the above equations, the “false positive, true positive, and the false negative” is shown by F^p , T^p and F^N respectively. The enhanced U-Net-based brain tumour segmentation is illustrated in Fig. 5.

4.3. Image Post-processing

Post-processing is used to eliminate undesirable bits from segmented

images of three regions such as enhancing tumour L_s^{enh} , whole tumour L_s^{who} , and core tumour L_s^{cor} , ensuring that the exact region of interest is extracted. Color balancing, sharpening, dynamic range compression, camera aberration correction, primary contrast adjustments, and more are all performed in post-processing. Post-processing aims to enhance the image quality generated by a lossy image compression system's decoder. These methods achieve high compression ratios, but they do so by discarding information that is deemed unimportant, causing distortion in the original image. The image is closed by a combination of dilatation and erosion. The incidence of dilatation and erosion process differs depending on the type of opening. In Eq. (26), (27), and (28), the link between dilatation and erosion is discussed.

$$L_s^{post} = (L_s^{enh} \oplus ME) - ME \quad (26)$$

$$L_s^{post} = (L_s^{who} \oplus ME) - ME \quad (27)$$

$$L_s^{post} = (L_s^{cor} \oplus ME) - ME \quad (28)$$

This closure procedure entails dilatation of the segmented image of the enhancing tumour L_s^{enh} , whole tumour L_s^{who} , and core tumour L_s^{cor} with ME as structuring factor, subsequent erosion by the same representation

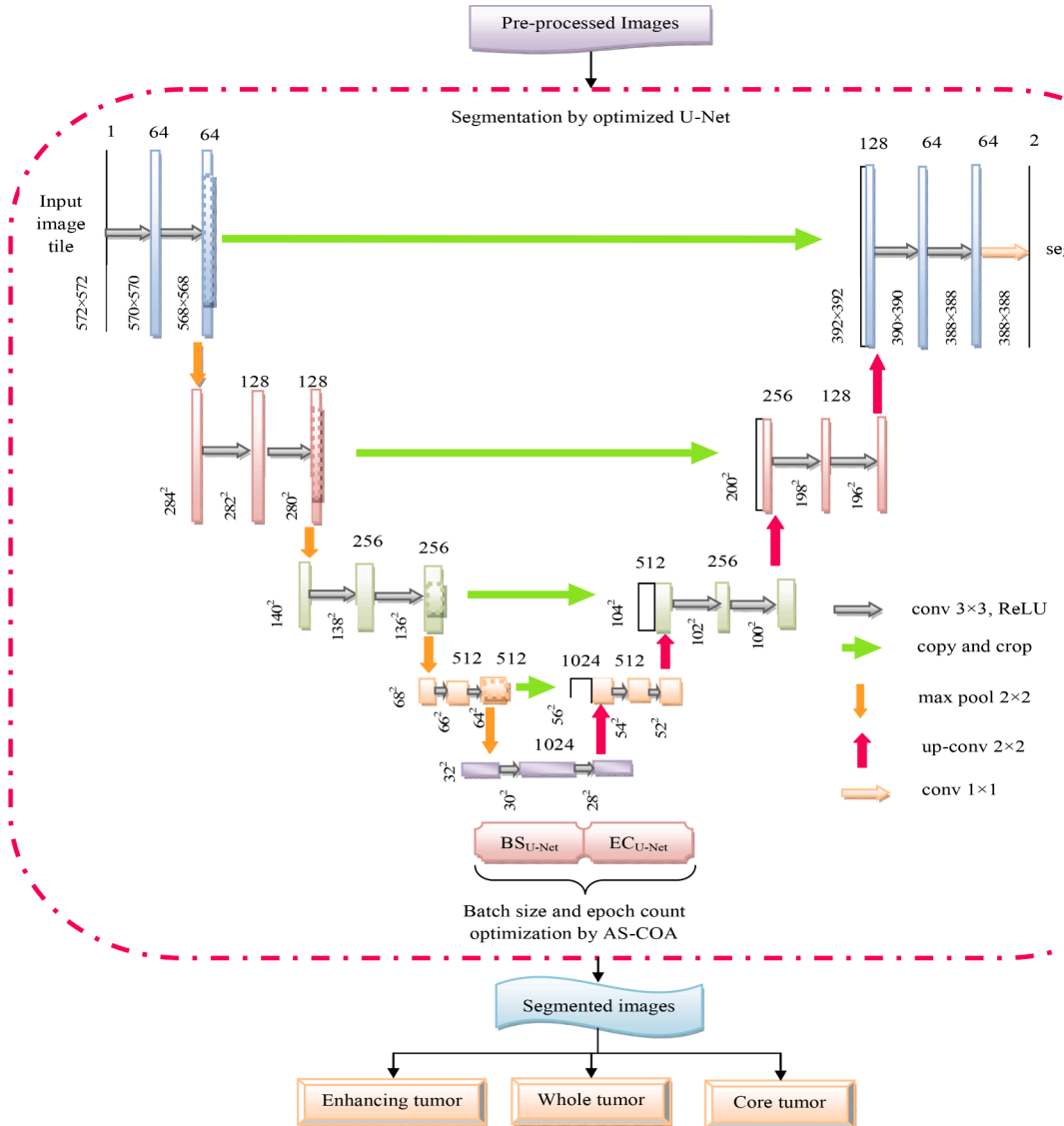


Fig. 5. Enhanced U-Net-based brain tumor segmentation model.

of element. Though the closure process smooths out parts of curves, it mostly combines minor fractures and thin gaps. Finally, minor flaws and gaps of object's edges are filled. Subsequently, the morphological closure procedure is used to get the post-processed images.

5. Results and discussions

5.1. Simulation setup

The proposed brain tumour segmentation model was simulated using Python, and the outcomes were assessed. The iteration counts and total

population were 10. The suggested AS-COA-EU-Net was performed against heuristic-based algorithms such as PSO-E-U-Net [30], GWO-E-U-Net [31], WOA-E-U-Net [32], COA-E-U-Net [26], and existing segmentation algorithms like FCM [33], K means [34] and U-Net [29] to describe the introduced model's superiority.

5.2. Performance metrics

The different performance metrics used here are as below.

(a) **Dice coefficient:** It is explained in Eq. (25).

(b) **Accuracy:** "the closeness of the measurements to a specific

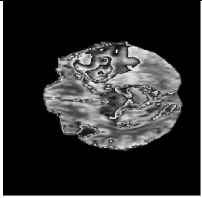
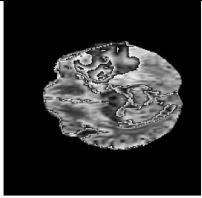
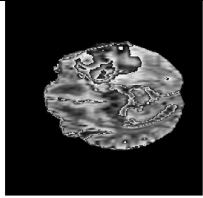
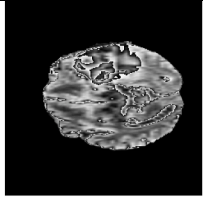

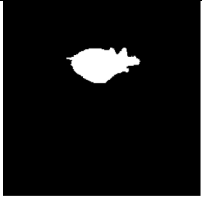




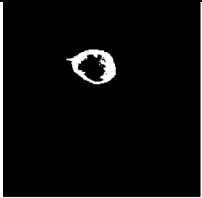

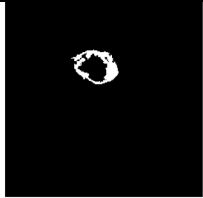
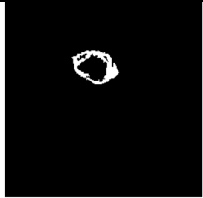

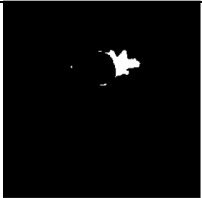

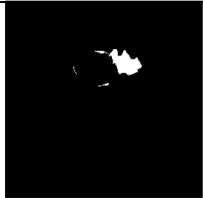
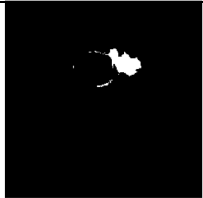
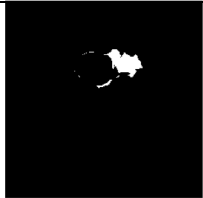
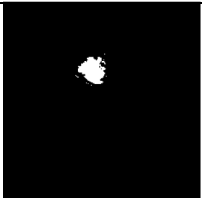

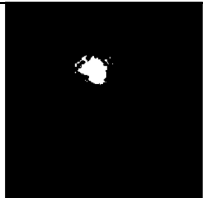
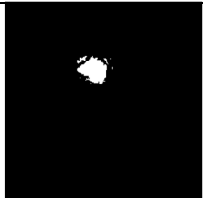
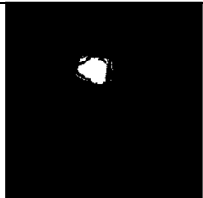
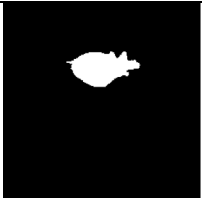


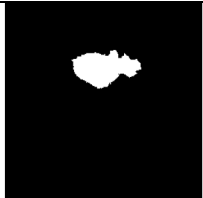

Sample images [35]	Image 1	Image 2	Image 3	Image 4	Image 5
Input image					
Ground truth image					
Enhancing tumour segmented image					
Whole tumour segmented image					
Core tumour segmented image					
Overall segmented image					

Fig. 6. Segmentation results for the introduced brain tumor segmentation model.

value”.

$$Accuracy = \frac{(T^p + T^n)}{(T^p + T^n + F^p + F^n)} \quad (29)$$

(c) Jaccard Coefficient: “It is a statistic used for gauging the similarity and diversity of sample images”.

$$Jaccard = \frac{T^p}{(T^p + F^p + F^n)} \quad (30)$$

(d) Precision: “the fraction of relevant instances among the retrieved instances”.

$$precision = \frac{T^p}{T^p + F^p} \quad (31)$$

(e) Sensitivity: “It refers to the correctly identified retrieved data among the various images”.

$$sensitivity = \frac{T^p}{T^p + F^n} \quad (32)$$

(f) Specificity: “It expresses the rate of the wrong data correctly neglected during the data retrieval”.

$$specificity = \frac{T^n}{F^p + T^n} \quad (33)$$

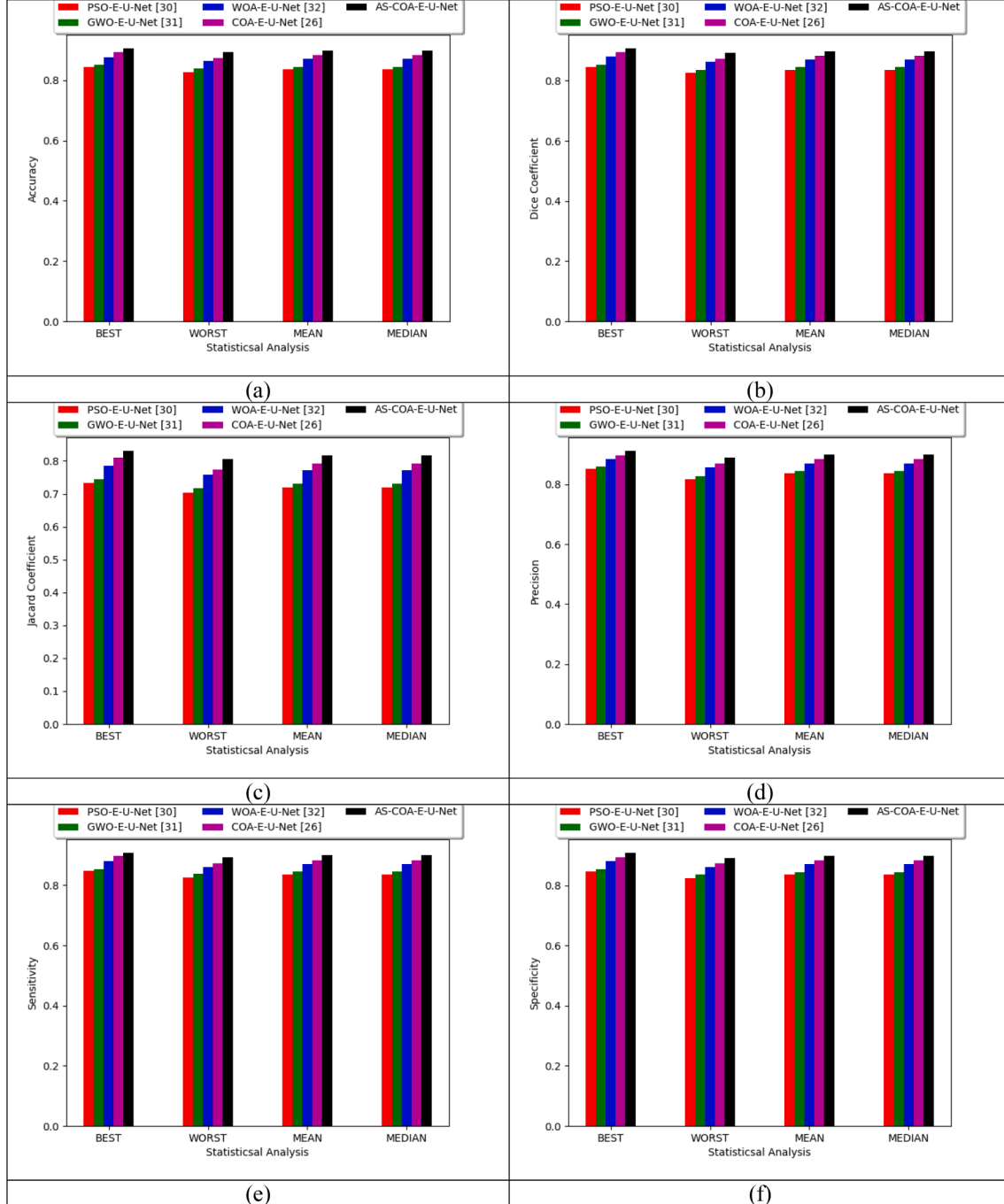


Fig. 7. Algorithmic Analysis of different heuristic-based algorithms for brain tumor segmentation model in terms of, “(a) Accuracy, (b) Dice coefficient, (c) Jaccard Coefficient, (d) Precision, (e) Sensitivity, and (f) Specificity”.

5.3. Segmentation results

The resultant images of segmentation model is attained using the enhanced U-Net are shown in Fig. 6.

5.4. Algorithmic analysis

Different algorithms are used for analyse the comparative performance for the brain tumour segmentation model is shown in Fig. 7. The outcomes demonstrate the betterment of the proposed AS-COA-E-U-Net. From Fig. 7(b), the dice coefficient of AS-COA-E-U-Net in terms of mean

is 2.25 %, 3.41 %, 8.33 %, and 9.64 % better than COA- E-U-Net, WOA- E-U-Net, GWO- E-U-Net, and PSO- E-U-Net correspondingly. Similarly, in the analysis of worst performance, the developed model seems to be enhanced in accurately extracting the brain tumor regions. Thus, the outcomes proved that the algorithmic analysis is better with AS-COA-E-U-Net for the brain tumour segmentation model.

5.5. Analysis of segmentation models

The segmentation model analysis of different existing segmentation-assisted techniques for the introduced brain tumour classification model

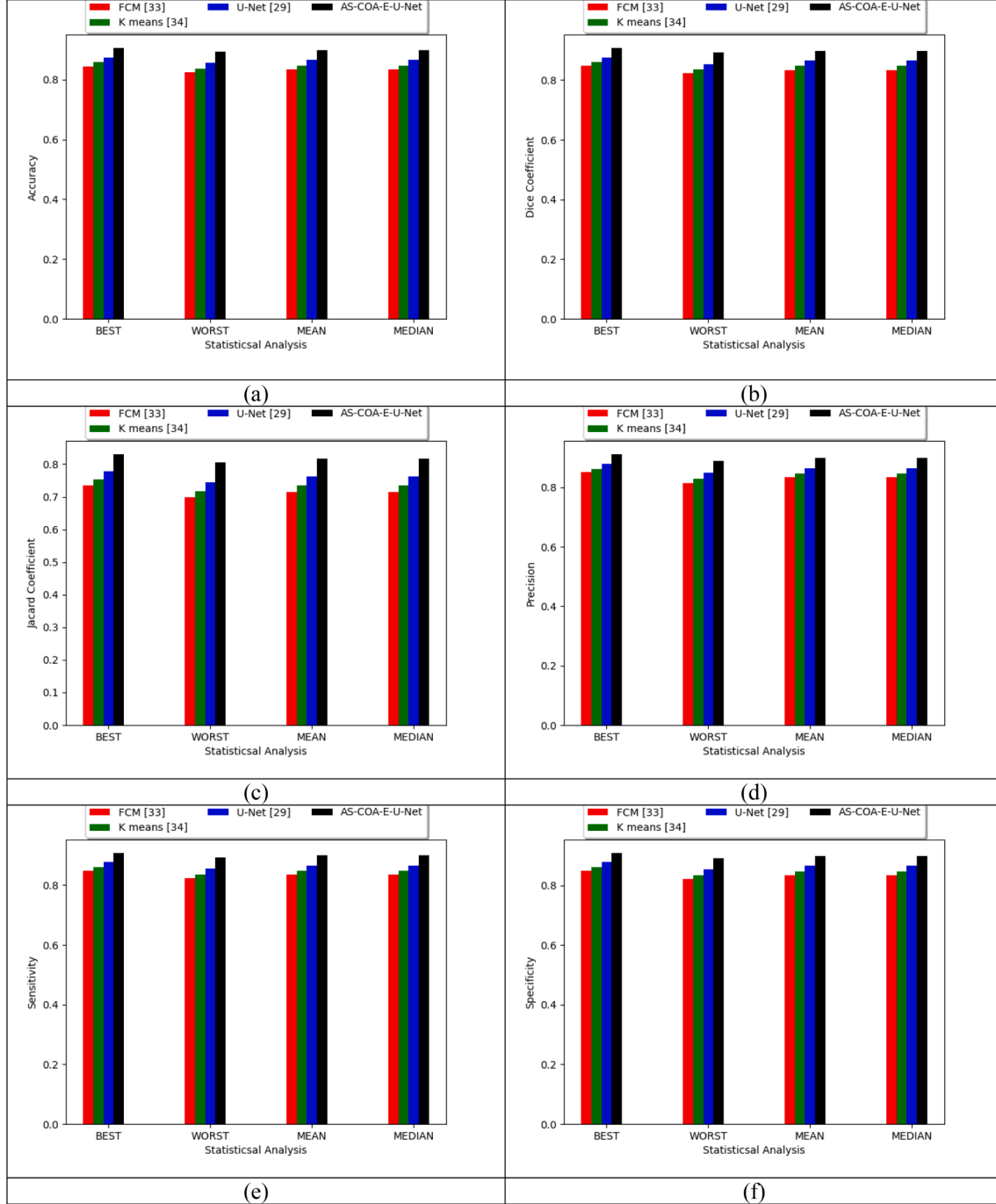


Fig. 8. Segmentation Model Analysis of different existing segmentation-based algorithms for brain tumor segmentation model in terms of, “(a) Accuracy, (b) Dice coefficient, (c) Jaccard Coefficient, (d) Precision, (e) Sensitivity, and (f) Specificity”.

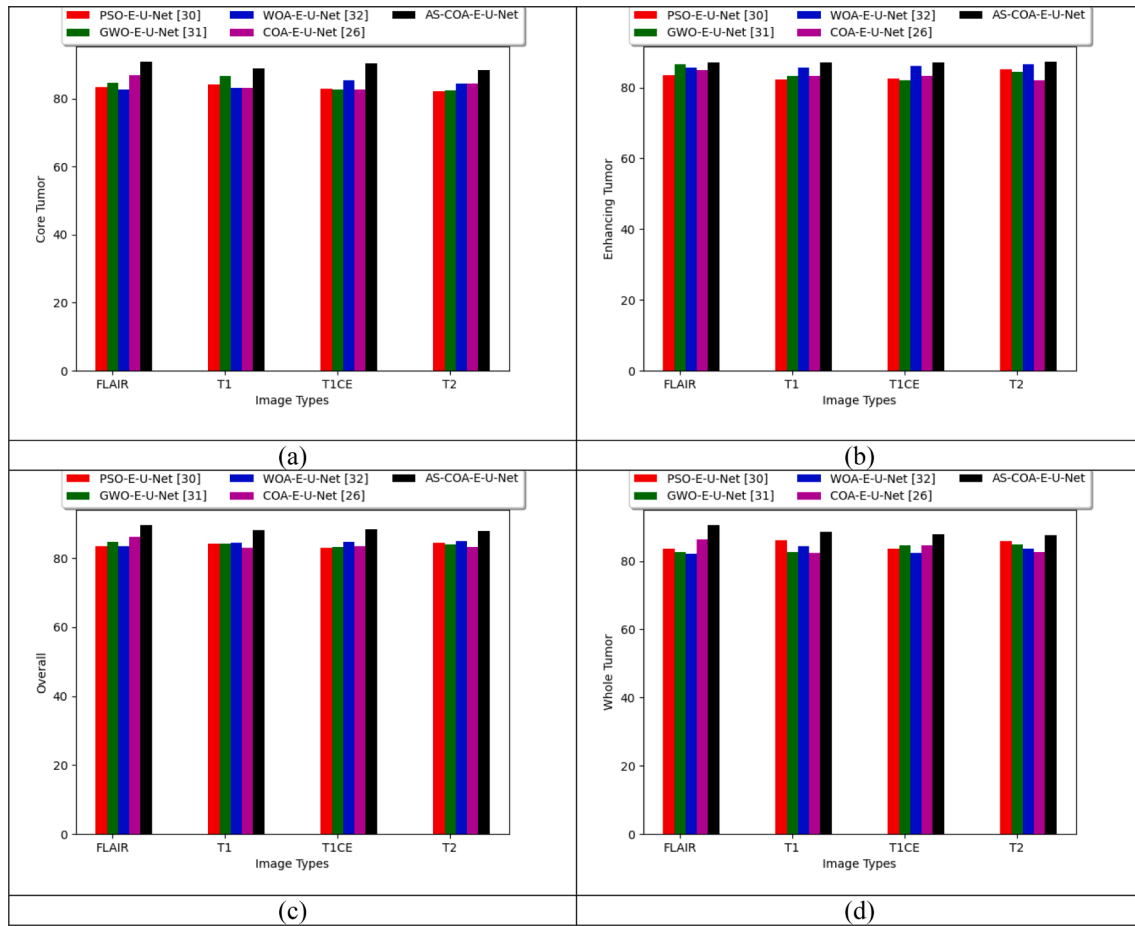


Fig. 9. Overall segmentation analysis for the developed brain tumor segmentation model in terms of “(a)core tumor, (b) enhancing tumor, (c) overall tumor and (d) whole tumor”.

utilizes distinct measures is shown in Fig. 8. It is clear from Fig. 8 that AS-COA- E-U-Net achieved better outcomes than the other methods. From Fig. 8(b), the dice coefficient of AS-COA- E-U-Net in terms of mean is 4.49 %, 6.90 %, and 8.14 % surpassing than U-Net, K means, and FCM respectively. Worst measure-based statistical analysis shows the improved brain tumor segmentation that is performed through the developed AS-COA-E-U-Net. Hence, the developed brain tumour segmentation model is better with AS-COA-E-U-Net than the other methods.

5.6. Overall segmentation analysis

The overall segmentation analysis of different heuristic-based algorithms in terms of “enhancing tumour, whole tumour, and the core tumour” is given in Fig. 9. The segmentation results are better with AS-COA-E-U-Net than the other methods in all the considered scans. In the case of FLAIR, the core tumour segmented output of AS-COA-E-U-Net is 3.96 %, 7.20 %, 5.77 %, and 7.17 % more advanced than COA- E-U-Net, WOA- E-U-Net, GWO- E-U-Net, and PSO- E-U-Net correspondingly. While considering T1, the whole tumour segmented output of AS-COA-E-U-Net is 6.29 %, 4.54 %, 4.73 %, and 4.70 % higher than COA- E-U-Net, WOA- E-U-Net, GWO- E-U-Net, and PSO- E-U-Net accordingly. In the case of T1 ce, the enhancing tumour segmented output of AS-COA-E-U-Net is 5.87 %, 4.48 %, 6.29 %, and 6.46 % superior to COA- E-U-Net, WOA- E-U-Net, GWO- E-U-Net, and PSO- E-U-Net correspondingly. Similarly, in T2, the overall segmented output of AS-COA-E-U-Net is 5.68 %, 3.48 %, 4.62 %, and 4.02 % progressed than COA- E-U-Net, WOA- E-U-Net, GWO- E-U-Net, and PSO- E-U-Net accordingly. Hence, the overall segmentation analysis is effective with AS-COA-E-U-Net than

classical approaches for the improved brain tumour segmentation model.

6. Conclusion

The main purpose of this paper was to explore a new deep learning-aided brain tumor segmentation model for MRI data. The input MRI images were given into pre-processing techniques like filtering and contrast enhancement methods, then patch extraction was processed. The Enhanced U-Net model performed image segmentation with pre-processed image, using the optimized AS-COA architecture. By solving the objective function as dice coefficient maximization, the key parameters of the U-Net architecture, such as batch size and epoch count, were optimized. The morphological closure model was used in the post-processing stage to retrieve the relevant region of having the greatest precision. Finally, the proposed approach calculated dice scores for the enhancing tumor, the whole tumor, and the core tumor. From the analysis, the whole tumour segmented output of AS-COA-E-U-Net was 6.29 %, 4.54 %, 4.73 %, and 4.70 % higher than COA- E-U-Net, WOA- E-U-Net, GWO- E-U-Net, and PSO- E-U-Net correspondingly. Hence, the overall analysis revealed that AS-COA-E-U-Net was better against traditional approaches for the developed brain tumour segmentation model.

Declaration of Competing Interest

The authors declare that they have no known competing financial interests or personal relationships that could have appeared to influence the work reported in this paper.

Data availability

Data will be made available on request.

References

- [1] S. Pereira, A. Pinto, V. Alves, C.A. Silva, Brain Tumor Segmentation Using Convolutional Neural Networks in MRI Images, *IEEE Transactions on Medical Imaging* 35 (5) (May 2016) 1240–1251.
- [2] W. Deng, Q. Shi, M. Wang, B. Zheng, N. Ning, Deep Learning-Based HCNN and CRF-RRNN Model for Brain Tumor Segmentation, *IEEE Access* 8 (2020) 26665–26675.
- [3] M. Ali, S.O. Gilani, A. Waris, K. Zafar, M. Jamil, Brain Tumour Image Segmentation Using Deep Networks, *IEEE Access* 8 (2020) 153589–153598.
- [4] M.I. Razzak, M. Imran, G. Xu, Efficient Brain Tumor Segmentation with Multiscale Two-Pathway-Group Conventional Neural Networks, *IEEE Journal of Biomedical and Health Informatics* 23 (5) (Sept. 2019) 1911–1919.
- [5] R. Thillaikkarasi and S. Saravanan, “An Enhancement of Deep Learning Algorithm for Brain Tumor Segmentation Using Kernel Based CNN with M-SVM,” *Journal of Medical Systems*, vol. 43, no. 84, 2019.
- [6] R. Pitchai, P. Supraja, A. Helen Victoria, M. Madhavi, “Brain Tumor Segmentation Using Deep Learning and Fuzzy K-Means Clustering for Magnetic Resonance Images,” *Neural, Processing Letters* 53 (2021) 2519–2532.
- [7] P. Ramya, M.S. Thanabal, C. Dharmaraja, Brain tumor segmentation using cluster ensemble and deep super learner for classification of MRI, *Journal of Ambient Intelligence and Humanized Computing* 12 (2021) 9939–9952.
- [8] M. Jiang, F. Zhai, J. Kong, A novel deep learning model DDU-net using edge features to enhance brain tumor segmentation on MR images, *Artificial Intelligence in Medicine* 121 (102180) (November 2021).
- [11] A. Hamamci, N. Kucuk, K. Karaman, K. Engin, G. Unal, Tumor-Cut: Segmentation of Brain Tumors on Contrast Enhanced MR Images for Radiosurgery Applications, *IEEE Transactions on Medical Imaging* 31 (3) (March 2012) 790–804.
- [12] A. Demirhan, M. Törü, İ. Güler, Segmentation of Tumor and Edema Along With Healthy Tissues of Brain Using Wavelets and Neural Networks, *IEEE Journal of Biomedical and Health Informatics* 19 (4) (July 2015) 1451–1458.
- [13] J.J. Corso, E. Sharon, S. Dube, S. El-Saden, U. Sinha, A. Yuille, Efficient Multilevel Brain Tumor Segmentation With Integrated Bayesian Model Classification, *IEEE Transactions on Medical Imaging* 27 (5) (May 2008) 629–640.
- [14] B. Yu, et al., SA-LuT-Nets: Learning Sample-Adaptive Intensity Lookup Tables for Brain Tumor Segmentation, *IEEE Transactions on Medical Imaging* 40 (5) (May 2021) 1417–1427.
- [15] D. Zhang, et al., Exploring Task Structure for Brain Tumor Segmentation From Multi-Modality MR Images, *IEEE Transactions on Image Processing* 29 (2020) 9032–9043.
- [16] T. Imtiaz, S. Rifat, S.A. Fattah, K.A. Wahid, Automated Brain Tumor Segmentation Based on Multi-Planar Superpixel Level Features Extracted From 3D MR Images, *IEEE Access* 8 (2020) 25335–25349.
- [17] W. Shan Shen, M.G. Sandham, A. Sterr, MRI fuzzy segmentation of brain tissue using neighborhood attraction with neural-network optimization, *IEEE Transactions on Information Technology in Biomedicine*, Sept. 9 (3) (2005) 459–467.
- [18] M.B. Cuadra, C. Pollo, A. Bardera, O. Cuisenaire, J., . Villemure and J. -. Thiran, “Atlas-based segmentation of pathological MR brain images using a model of lesion growth,” *IEEE Transactions on Medical Imaging*, Oct. 23 (10) (2004) 1301–1314.
- [19] A. Gooya, et al., GLISTR: Glioma Image Segmentation and Registration, *IEEE Transactions on Medical Imaging* 31 (10) (Oct. 2012) 1941–1954.
- [20] S. Zhou, D. Nie, E. Adeli, J. Yin, J. Lian, D. Shen, High-Resolution Encoder–Decoder Networks for Low-Contrast Medical Image Segmentation, *IEEE Transactions on Image Processing* 29 (2020) 461–475.
- [21] T. Zhou, S. Canu, P. Vera, S. Ruan, Latent Correlation Representation Learning for Brain Tumor Segmentation With Missing MRI Modalities, *IEEE Transactions on Image Processing* 30 (2021) 4263–4274.
- [22] M.S. Majib, M.M. Rahman, T.M.S. Sazzad, N.I. Khan, S.K. Dey, VGG-SCNet: A VGG Net-Based Deep Learning Framework for Brain Tumor Detection on MRI Images, *IEEE Access* 9 (2021) 116942–116952.
- [23] H. Mzoughi, I. Njeh, Mohamed Ben Slima, Ahmed Ben Hamida, Chokri Mhiri and Kheireddine Ben Mahfoudh, “Towards a computer aided diagnosis (CAD) for brain MRI glioblastomas tumor exploration based on a deep convolutional neuronal networks (D-CNN) architectures,” *Multimedia Tools and Applications* 80 (2021) 899–919.
- [24] H. Mzoughi, I. Njeh, A. Wali, M.B. Slima, A.B. Hamida, C. Mhiri, K.B. Mahfoudhe, Deep Multi-Scale 3D Convolutional Neural Network (CNN) for MRI Gliomas Brain Tumor Classification, *Journal of Digital Imaging* 33 (2020) 903–915.
- [25] B. Srinivas, G.S. Rao, “Segmentation of Multi-Modal MRI Brain Tumor Sub-Regions Using Deep Learning,” *Journal of Electrical, Engineering & Technology* 15 (2020) 1899–1909.
- [26] Z. Yuan, W. Wang, H. Wang, A. Yildizbasi, Developed Coyote Optimization Algorithm and its application to optimal parameters estimation of PEMFC model, *Energy Reports* 6 (November 2020) 1106–1117.
- [27] Derry FitzGerald and Kevin St, “HARMONIC/PERCUSSIVE SEPARATION USING MEDIAN FILTERING”, *Proc. of the 13th Int. Conference on Digital Audio Effects (DAFx-10)*, Graz, Austria , September 6–10, 2010.
- [28] H. Yeganeh, A. Ziaei, A. Rezaie, A Novel Approach for Contrast Enhancement Based on Histogram Equalization, *Kuala Lumpur, Malaysia*, 2008.
- [29] Olaf Ronneberger, Philipp Fischer, and Thomas Brox, “U-Net: Convolutional Networks for Biomedical Image Segmentation”, *Springer*, pp. 234–241, 2015.
- [30] V. Thambusamy, Detection of Brain Tumor by Particle Swarm Optimization using Image Segmentation, *Indian Journal of Science and Technology* 8 (22) (August 2015).
- [31] A. Geetha, N. Gomathi, A robust grey wolf-based deep learning for brain tumour detection in MR images, *Biomedizinische Technik/Biomedical Engineering* 65 (2) (October 2019).
- [32] T. Vaiyapuri, A. Haya, Whale Optimization for Wavelet-Based Unsupervised Medical Image Segmentation: Application to CT and MR Images, *International Journal of Computational Intelligence Systems* 13 (1) (July 2020).
- [33] P. Vasuda, S. Satheesh, Improved Fuzzy C-Means Algorithm for MR Brain Image Segmentation, *International Journal on Computer Science and Engineering* 2 (5) (August 2010).
- [34] Amjad Rehman, Siraj Khan, Majid Harouni, and Rashid Abbasi, “Brain tumor segmentation using K-means clustering and deep learning with synthetic data augmentation for classification”, *Microscopy Research and Technique*, February 2021.
- [35] <https://www.kaggle.com/aryashah2k/brain-tumor-segmentation-brats-2019>.